HHS Public Access

Author manuscript

Nat Commun. Author manuscript; available in PMC 2016 May 20.

Published in final edited form as:

Nat Commun. ; 6: 8919. doi:10.1038/ncomms9919.

C. elegans maximum velocity correlates with healthspan and is maintained in worms with an insulin receptor mutation

Jeong-Hoon Hahm[1], **Sunhee Kim**[1,#], **Race DiLoreto**[2,#], **Cheng Shi**[2,#], **Seung-Jae V. Lee**[3], **Coleen T. Murphy**[2,*], and **Hong Gil Nam**[1,4,*]

[1]Center for Plant Aging Research, Institute for Basic Science, Daegu, 42988, Republic of Korea

[2]Department of Molecular Biology, Lewis-Sigler Institute for Integrative Genomics, Princeton University, 148 Carl Icahn Laboratory, Washington Road, Princeton, New Jersey 08544, USA

[3]Department of Life Sciences and School of Interdisciplinary Bioscience and Bioengineering, Pohang University of Science and Technology, Pohang, Gyeongbuk, 790-784, Republic of Korea

[4]Department of New Biology, DGIST, Daegu, 42988, Republic of Korea

Abstract

Aging is marked by physical decline. *C. elegans* is a valuable model for identifying genetic regulatory mechanisms of aging and longevity. Here we report a simple method to assess *C. elegans'* maximum physical ability based on the worms' maximum movement velocity. We show maximum velocity declines with age, correlates well with longevity, accurately reports movement ability, and, if measured in mid-adulthood, is predictive of maximal lifespan. Contrary to recent findings, we observe that maximum velocity of worm with mutations in *daf-2(e1370)* insulin/IGF-1 signaling scales with lifespan. Because of increased odorant receptor expression, *daf-2(e1370)* mutants prefer food over exploration, causing previous on-food motility assays to underestimate movement ability and, thus, worm health. Finally, a disease-burden analysis of published data reveals that the *daf-2(e1370)* mutation improves quality of life, and therefore combines lifespan extension with various signs of an increased healthspan.

Aging is an important risk factor for disease and is accompanied by the decline of many physiological characteristics, including physical performance, negatively affecting quality of life. Therefore, quality of life with age, not just longevity, is important for our aging society. *C. elegans* has been a valuable model organism in revealing the genetic regulatory mechanisms of aging and longevity[1, 2]. One of the best-studied longevity pathways is the insulin/IGF-1 signaling (IIS) pathway, which regulates longevity in response to nutrient levels through its control of the activity of the FOXO transcription factor and its downstream targets[3, 4, 5, 6]. Mutations of the DAF-2 insulin receptor, particularly the canonical allele *daf-2(e1370)*, double lifespan[3] and extend the abilities to learn and

[*]Correspondence should be addressed to H.G.N. (nam@dgist.ac.kr) or C.T.M. (ctmurphy@Princeton.EDU).
[#]S.K., R.D. and C.S. contributed equally to this work.

The authors have no conflicts of interest to declare.

remember, resist stress and infection, repair axons[7], and suppress neuronal morphological defects[8, 9, 10] with age. The components of the IIS pathway are well-conserved, and are linked to extreme longevity in humans[11], as well. Recently, despite the fact that the *daf-2* mutation extends many physiological functions with age[7, 8, 9, 10], Bansal, et al. concluded that *daf-2(e1370)* insulin/IGF-1 signaling (IIS) mutants are less healthy than wild-type animals, disproportionately extending their "unhealthy" lifetime[2, 12].

One of the most powerful tests of physical ability in elderly humans is the Short Physical Performance Battery (SPPB)[13], an assessment of the maximum exercise capacity of lower extremities over a short period of time. The SPPB accurately predicts risk of disability[14], length of hospital stay, and mortality over the year after hospital discharge[15]. The SPPB includes a short (4 m) walk to measure maximum gait speed. Like humans, *C. elegans* shows age-related decline in physical ability, which is manifested by reduced body movement[16, 17, 18, 19, 20, 21, 22]. We wondered whether a similar metric of maximum velocity (MV) in a short period (30 s) would be equally informative in *C. elegans*. We found that worms' MV declines with age, correlates well with longevity, accurately reports movement ability, and importantly, is predictive of future longevity. *daf-2(e1370)* mutations extend MV and "healthspan", scaling with lifespan[19]. Motility assays performed on bacteria underestimate *daf-2(e1370)* mutants' movement ability due to their high *odr-10* levels and subsequent preference for food over exploration. We used human disease burden models to assess *C. elegans* mutants' quality of life; quality-adjusted re-analysis of data from previously-published healthspan studies[1, 2, 19] demonstrates that *daf-2(e1370)* mutants' healthspan correlates with longevity extension, and in terms of disease-burden analysis, improves quality of life. The IIS pathway mutation *daf-2(e1370)* coordinates the extension of lifespan with many aspects of healthspan, providing valuable insight into mechanisms that extend functional health with age.

Results

Maximum Velocity correlates with lifespan

To mimic the SPPB test used to assess health in elderly humans, we measured worms' maximum velocity (MV) over 30s on an unseeded NGM plate each day of adulthood (Supplementary Fig. 1). Our assay differs from previous motility assays in its brevity (30s vs 5 min[21] or longer[23]), longitudinal testing of individual worms rather than populations, and measurement on plates without bacteria[2]. MV appears to not simply be a response to harsh touch, as harsh touch mutants behave like wild-type worms in the assay, and the MV is distributed over the entire 30s window for all animals (Supplementary Fig. 2).

To assess age-associated decline of physical performance, we measured MV of 52 individual wild type worms each day of their lifespan (Fig. 1a). We found that motility decreased with age (Supplementary Fig. 3), with MV declining earlier and more drastically than mean velocity (Supplementary Fig. 3). During the early phase of adulthood (Day 1–5), MV of individual worms was maintained in the range of 0.22–0.52 mm/s. However, from Day 6 onwards, all worms showed a decline in MV with age.

We grouped worms into high (≥ 0.22 mm/s) and low (≤ 0.21 mm/s) MVs; the criterion was based on the minimum MV at Day 1 of adulthood. The population of the low MV group increased almost exponentially, reaching 54.6% by Day 9 of adulthood (Supplementary Fig. 4). We then examined the correlation between MV of worms at Day 9 of adulthood (mid-life) and their lifespan thereafter. Day 9 MV correlated well with lifespan (coefficient of determination (r^2) = 0.71), better than the correlation between lifespan and mean velocity (r^2 = 0.44; Fig. 1b,c), thrashing rate (r^2 = 0.18; Supplementary Fig. 5) or pharyngeal pumping (r^2 = 0.65; Supplementary Fig. 5). Remarkably, the median lifespan of worms in the Day 9 High MV group (23 ± 3.2 days) was 35.3% longer than that of the worms in the Day 9 Low MV group (17 ± 3.6 days; Fig. 1d). Thus, MV of wild-type worms at Day 9 of adulthood is a reliable predictor of longevity thereafter.

In humans, mitochondrial defects are associated with aging of skeletal muscle and are correlated with reduced physical strength in the elderly[24, 25, 26]. Young *C. elegans'* mitochondria are tubular[27]; however, gradual fragmentation with age results in sparse, globular mitochondria (Supplementary Fig. 6). At Day 9 of adulthood, worms in the low MV range had very fragmented mitochondria, while the high MV range group's mitochondria were significantly less damaged at the same age (Fig. 1e and Supplementary Fig. 7). Additionally, expression of the protective lifespan biomarker *sod-3*[28] was 1.69-fold higher in the high MV group than in the low MV group (Supplementary Fig. 8). These data show that MV correlates with two age-associated physiological parameters, and suggest that mechanisms determining MV might also regulate mitochondrial integrity maintenance and stress protection gene expression.

daf-2(e1370) mutation extends healthspan

We next assessed the MV of long-lived *daf-2(e1370)* Insulin/IGF-1 receptor mutants and short-lived mutants of the DAF-16 FOXO transcription factor (*daf-16(mu86))*, which is required for *daf-2* mutants' longevity[3, 4, 29] (Fig. 2a). *daf-2* animals exhibited a higher MV with age, particularly from Day 10 onward (Fig. 2b–d). At Day 26 of adulthood, when all the wild-type worms had died, *daf-2* mutants still maintained on average 36% of MV (Fig. 2d). We examined the correlation of MV on each day with the lifespan for the worms in the longitudinally tracked cohort (Figs 1a, 2b,c). The correlation between MV and lifespan is best on day 9 for N2 worms, day 23 for *daf-2*, and day 10 for *daf-16* (Supplementary Fig. 9); in all cases, the best correlation between MV and lifespan occurs within 1 day of the first death in the cohort. We integrated the area under the MV curve to serve as an indicator of overall physical performance; *daf-2* mutants showed a 2.4-fold increase over wild type, and *daf-16* mutants showed slightly lower physical performance (Fig. 2e). Thus, *daf-2(e1370)* mutation extends physical ability with age.

We then used MV to determine the "healthspan" (defined as the period with >50% of maximal activity[2]) and "gerospan" (period with <50% maximal activity[2]) ratios of wild-type, *daf-16(mu86)*, and *daf-2(e1370)* mutant worms, in the same manner as Bansal, et al[2]. While this type of analysis does not include any error calculation, our results suggest that *daf-2* mutants increased healthspan more than two-fold compared to wild type and *daf-16* mutants (Fig. 2f), and the resulting normalized healthspan-to-gerospan ratios were similar

among the three strains (Fig. 2g). Thus, *daf-2(e1370)* mutation extends both lifespan and healthspan to a similar extent, without proportionally extending the unhealthy part of life, in contrast to Bansal, et al.'s conclusions[2].

odr-10 levels determine on-food motility rates

We were concerned that differences in motility assays may have led to discrepancies with the previous report[2]. Our assay measures MV on plates without bacteria, while Bansal, et al. measured the distance worms moved on bacteria[2]. We wondered whether *daf-2's* lower motility on food might not reflect its ability to move, but rather its preference for food over exploration. Food-seeking preference is determined by levels of the odorant receptor *odr-10*[30]; high levels of *odr-10* suppress food-exploration behavior[30]. Ryan, et al. (2014) showed that *odr-10*, despite the fact that it is only expressed in the AWA neurons and primarily detects diacetyl, plays a major role in food detection and is the primary factor in determining the decision of males to explore (mate search) rather than feed[30]. Indeed, we found that the expression of *odr-10*, which contains a DAF-16 Binding Element (DBE) 809 bp upstream of its start site, is elevated 15–20-fold in *daf-2(e1370)* mutants (Fig. 3a). Furthermore, we observed that reduction of *odr-10* levels dramatically increases *daf-2's* motility on bacteria: unlike control-treated animals, which stop moving after 1.5-3 min when placed onto bacteria, *daf-2(e1370);odr-10(RNAi*) worms continue to move constantly over a 10 min assay period (Fig. 3b), and reduction of wild-type worms' *odr-10* levels has no significant effect (Fig. 3c and Supplementary Movies 1–3). (Interestingly, knockdown of other genes involved in odor detection, including *odr-3*, *odr-7*, and *osm-9*, did not have the same effect on *daf-2(e1370)* motility (Supplementary Fig. 10).) Therefore, motility can only accurately be measured off food, because movement on bacteria measures food-seeking rather than ability to move.

daf-2(e1370) mutation increases quality of life

As MV is only one metric of healthspan, we re-analyzed the entire Bansal, et al. healthspan dataset[2]. (The same *daf-2* allele, *e1370*, was used in their studies, as well.) In our analysis, we normalized each health metric at each timepoint to the maximum score of wild type to directly compare performance levels (Fig. 4a). This re-analysis shows that *daf-2* mutants were healthier than wild type in all metrics except thrashing in liquid. However, previous thrashing measurements of *daf-2* mutants[31] and another long-lived IIS mutant, *age-1*[32], demonstrate that these IIS mutants maintain thrashing activity with age better than wild type.

We wondered whether cost-utility (disease burden) methods developed to assess quality of life[33] (which are typically used to make cost assessments of human disease treatment options) could be applied to these healthspan analyses of *C. elegans*. To do so, we combined information from the lifespan curve and health measurements reported by Bansal et al. to obtain a "quality-adjusted lifespan" curve, according to the method of Zeckhauser & Shepard[33]. We multiplied the lifespan curve by the normalized healthspan curve, producing a curve that describes both the declining health of the animal and the declining survival of the population (Fig. 4b). By calculating the area under the curve (AUC) of the quality-adjusted lifespan, we can visualize total quality of life, taking into account both survival and

health (Fig. 4c) (Methods). Re-analysis of the Bansal, et al. data[2] using this approach suggests that while not all longevity mutants have a commensurate increase in life quality (in fact, some longevity mutants, such as *clk-1*, exhibit lower total quality, as Bansal, et al. reported), increased health and extended lifespan result in a higher total quality for *daf-2(e1370)* mutants. (We note that the cumulative quality-adjusted score for thrashing is equivalent for *daf-2(e1370)* and wild type, but that thrashing has little correlation overall with longevity (Supplementary Fig. 5).) We reached a similar conclusion upon re-analysis of the data from Huang, et al.[19], which also measured several healthspan parameters (Fig. 4d and Supplementary Fig. 11a,b). Additionally, applying this analysis to our own MV data shows the same dramatic increase in *daf-2(e1370)* lifespan quality (Supplementary Fig. 11c–e). Thus it appears from multiple analyses of healthspan that *daf-2(e1370)* mutants have a higher quality of life than wild-type worms.

Discussion

Here we have modeled the SPPB assessment of physical ability in elderly humans in worms, using a simple assay of *C. elegans'* maximum ability to move over a short period. MV correlates well with age; in fact, MV performance at mid-life (day 9) can predict the remaining lifespan of the individual. Our analysis also reveals that other widely-used healthspan metrics are less correlated with lifespan; thrashing is a particularly poor correlate (r^2= 0.18), while pumping has a good correlation (r^2= 0.65) but shows highly irregular patterns (Supplementary Fig. 5). Thus, maximum velocity is a powerful healthspan proxy and may be the most informative metric of *C. elegans'* health with age.

An unexpected benefit of this experimental design is that it is not confounded by the worms' ongoing assessment of its bacterial food source. We discovered that *daf-2* has an inherently higher preference for food than exploration, likely due to its increased expression level of the *daf-2/daf-16* target *odr-10*; high levels of the ODR-10 odor receptor cause *daf-2* worms to prefer food over exploration, slowing its movement on bacteria. (Further, our data on other chemosensory genes suggest that *odr-10* is a particularly good indicator of food preference.) Because this type of movement is not limited by ability, but rather by preference, it may be difficult to draw conclusions regarding healthspan from on-food motility assays.

Measurements that take into account both lifespan and healthiness are important in assessing quality of life with age, and the clinical implications of coordinated extension of lifespan and healthspan are immense. Not all lifespan interventions will improve health or total quality, as *clk-1* mutants demonstrate. In fact, several longevity mutants are less healthy overall than wild-type worms by different measurements, and it is important to note which mutants may have a long life with no health benefit. However, we find no evidence to support Bansal, et al.'s claim that *daf-2(e1370)* mutants spend a greater fraction of life in a frail state; in fact, *daf-2* mutants demonstrate that healthspan and lifespan can be coordinately extended. From the analysis of our own data and that of published experiments, it seems clear that *daf-2* extends not only lifespan, but also many abilities with age. In addition to the standard *C. elegans*-specific "healthspan" assays (heat stress, oxidative stress, movement), *daf-2* extends behaviors that are relevant for human decline with age, as

well. This includes the abilities to learn and remember[34], repair axons[7], resist pathogenic infections[35], suppress age-related neuronal morphological defects[8, 9, 10] and neurodegenerative protein aggregation[36], maintain neuromuscular junction activity[23, 37], and maintain high-quality oocytes with age[38]. Many of the downstream targets of the *daf-2* insulin signaling pathway[6] that enable these functions have been identified, and many of these genes and the underlying mechanisms are conserved in mammals; therefore, the extended abilities that *daf-2* exhibits offers therapeutic target possibilities.

Defining “healthspan” and “gerospan” based on population maximum lifespans ignores the fact that quality is a continuum. Instead, our analysis takes into account the length of time an individual can expect to live, and how healthy that individual can expect to be with age. In the case of *daf-2(e1370)* mutants, quality of life is clearly superior. The mechanistic study of coordinated health and life extension might allow the development of therapeutics to remedy end-of-life problems or to compress morbidity, decreasing health costs. *C. elegans* IIS longevity mutants remain valuable tools in understanding the mechanisms by which we might achieve these goals.

METHODS

Strains

The *C. elegans* strain, N2 Bristol, was used as the wild type. The N2 strain and the insulin/IGF-1 mutants, *daf-2(e1370)*, *daf-16(mu86)*, CF1553 *muIs84*[pAD76 *(sod-3::GFP)*] and PD4251 ccIs4251 I; *dpy-20(e1282)* IV were obtained from the *Caenorhabditis* Genetics Center (CGC).

Measurement of worm maximum velocity (MV)

Synchronized worms were prepared by placing adult worms on a Nematode Growth Medium (NGM) plate and allowing them to lay eggs for 3 h. After removing the adult worms, each synchronized progeny was transferred to a single NGM plate and cultured to L4 stage. After 24 h, single worms were transferred to the physical assay plate and movements recorded immediately. The assay conditions were as follows: 20°C and ~40% humidity, with no lid. The physical assay plate was prepared in the same manner as the NGM, but with no bacterial lawn. The recording system comprised a stereomicroscope (Nikon SMZ 745T), a CCD camera (TUCSEN TCH-5.0), and imaging software (TUCSEN ISCapture). A 12.14× zoom lens was used to keep the worms within the field of view. Movement was recorded every 24 h throughout the lifespan of each worm. The recording period was 30 seconds at a rate of 30 frames per second. After recording, the worm was transferred to a fresh NGM plate (the ‘growth plate’ shown in Supplementary Fig. 1). The locomotion velocity was expressed as mm/s (the distance (mm) between displaced centroids per second). Recorded images were analyzed by ImageJ and wrMTrck (plugin for ImageJ: www.phage.dk/plugins). The locomotion velocity data were imported into an Excel spreadsheet. The peak locomotion velocity observed in the 30 seconds period was used as the MV.

Lifespan analysis

Lifespan was assessed on NGM plates at 20°C. The number of live animals was scored every day until death. Lifespan was analyzed by Oasis survival analysis software[39].

Pharyngeal pumping and thrashing rate decline assays

Synchronized single worms were observed every day. The number of contractions in the terminal bulb of pharynx was counted for 30 seconds (n = 19). The change in the reciprocating motion of bending at the mid-body in S-basal medium was counted as a body bend. The number of body bends was counted for 30 seconds (n = 20).

Qualitative analysis of mitochondrial morphology

Morphological categories were defined according to Regmi[27]: (1) images showing a majority of long interconnected mitochondrial networks were classified as tubular; (2) images showing a combination of interconnected mitochondrial networks along with some smaller fragmented mitochondria were classified as intermediate; (3) images showing a majority of short mitochondria were classified as fragmented; and (4) images showing sparse globular mitochondria were classified as very fragmented. We scored mitochondrial morphology as ‘1’ (very fragmented), ‘2’ (fragmented), ‘3’ (intermediate) and ‘4’ (tubular) (Supplementary Fig. 7). Mitochondrial morphology was examined in PD4251 strains at Day 9 of adulthood after MV was recorded. Worms were immobilized during imaging using 30mM sodium azide. Imaging was performed using a microscope equipped with a C-Apochromat 40x/1.20W Korr FCS M27 and a photo-multiplier tube (PMT). Zen 2011software (black edition) was used to acquire fluorescent z stacks of individual animals (1μm/slice).

Observation of *sod-3* expression

sod-3 expression was examined in CF1553 strain worms at Day 9 of adulthood after MV was recorded. Imaging was performed using a microscope equipped with a C-Apochromat 10x/1.20W Korr FCS M27 and a photo-multiplier tube (PMT). Zen 2011software (black edition) was used to acquire fluorescent z stacks of individual animals (1μm/slice). Worms were immobilized during imaging using 30mM sodium azide.

odr-10 qRT-PCR measurements

Two sets of primers (#1 and #2) were used to measure the expression of *odr-10* by qRT-PCR in N2 and *daf-2* mutants. For each primer set, *odr-10* expression in wild type was normalized to 1. *pmp-3* was used as a reference gene.

“odr-10-qRT-1-r” 5′ – AAC GGT GCG ATG AAC ATG AC – 3′

“odr-10-qRT-1-f” 5′ – CTT CAG GTA TCC CGA TCT GAA ACT – 3′

“odr-10-qRT-2-r” 5′ – TCA GAT CGG GAT ACC TGA AGA – 3′

“odr-10-qRT-2-f” 5′ – TCT ACT GCG GAT ATG CCA CG – 3′

Reference gene primers: *pmp-3*

Forward: AGTTCCGGTTGGATTGGTCC

Reverse: CCAGCACGATAGAAGGCGAT

Quality-adjusted lifespan analysis

Quality metrics were taken from published work. Because the raw data from Bansal, et al.,[2] were not made publicly available by the authors at time of submission of this paper, we extracted data from their figures using GetData Graph Digitizer. (No N or error information is available, however.) The lifespan (L(t)) (% surviving with age) and healthspan (H(t)) (health measurement with age) data were graphed using a left-hand step function. The curves were combined by multiplying the lifespan and healthspan curves together, with the value of the resulting quality-adjusted lifespan curve (Q(t)) being Q(t) = L(t) * H(t). The area under the curves was calculated by taking the definite integral of this step function. The set of timepoints T is zero-indexed and consists of $T=\{t_0,t_1,\ldots,t_n\}$, and we calculate the area under the curve as shown in equation (1).

$$AUC=\sum_{i=1}^{n} Q(t_i) \times (t_i - t_{i-1}) \quad (1)$$

Supplementary Material

Refer to Web version on PubMed Central for supplementary material.

Acknowledgments

We thank the *Caenorhabditis* Genetics Center (CGC) for strains. The authors are grateful to Prof. Jan Vijg, Prof. Yousin Suh, and Prof. Kyuhyung Kim for their valuable suggestions. This work was supported by the Research Center Program of the Institute for Basic Science (project code: IBS-R013-D1) and the National Institutes of Health (Grant number 5T32GM007388-38). CTM is the Director of the Glenn Center for Aging Research at Princeton University. RD is supported by NIH 5T32GM007388-38, and CS by March of Dimes.

References

1. Kenyon CJ. The genetics of ageing. Nature. 2010; 464:504–512. [PubMed: 20336132]
2. Bansal A, Zhu LHJ, Yen K, Tissenbaum HA. Uncoupling lifespan and healthspan in Caenorhabditis elegans longevity mutants. Proc Natl Acad Sci U S A. 2015; 112:E277–E286. [PubMed: 25561524]
3. Kenyon C, Chang J, Gensch E, Rudner A, Tabtiang R. A C. elegans mutant that lives twice as long as wild type. Nature. 1993; 366:461–464. [PubMed: 8247153]
4. Ogg S, et al. The Fork head transcription factor DAF-16 transduces insulin-like metabolic and longevity signals in C-elegans. Nature. 1997; 389:994–999. [PubMed: 9353126]
5. Lin K, Hsin H, Libina N, Kenyon C. Regulation of the Caenorhabditis elegans longevity protein DAF-16 by insulin/IGF-1 and germline signaling. Nature genetics. 2001; 28:139–145. [PubMed: 11381260]
6. Murphy CT, et al. Genes that act downstream of DAF-16 to influence the lifespan of Caenorhabditis elegans. Nature. 2003; 424:277–283. [PubMed: 12845331]
7. Byrne AB, Walradt T, Gardner KE, Hubbert A, Reinke V, Hammarlund M. Insulin/IGF1 signaling inhibits age-dependent axon regeneration. Neuron. 2014; 81:561–573. [PubMed: 24440228]
8. Toth ML, et al. Neurite sprouting and synapse deterioration in the aging Caenorhabditis elegans nervous system. The Journal of neuroscience. 2012; 32:8778–8790. [PubMed: 22745480]
9. Tank EM, Rodgers KE, Kenyon C. Spontaneous age-related neurite branching in Caenorhabditis elegans. The Journal of neuroscience. 2011; 31:9279–9288. [PubMed: 21697377]

10. Pan CL, Peng CY, Chen CH, McIntire S. Genetic analysis of age-dependent defects of the Caenorhabditis elegans touch receptor neurons. Proc Natl Acad Sci U S A. 2011; 108:9274–9279. [PubMed: 21571636]
11. Barzilai N, Gabriely I, Atzmon G, Suh Y, Rothenberg D, Bergman A. Genetic studies reveal the role of the endocrine and metabolic systems in aging. The Journal of clinical endocrinology and metabolism. 2010; 95:4493–4500. [PubMed: 20926537]
12. Bansal A, Tissenbaum HA. Quantity or Quality?. 2015
13. Guralnik JM, et al. A short physical performance battery assessing lower extremity function: association with self-reported disability and prediction of mortality and nursing home admission. Journal of gerontology. 1994; 49:M85–94. [PubMed: 8126356]
14. Studenski S, et al. Physical performance measures in the clinical setting. Journal of the American Geriatrics Society. 2003; 51:314–322. [PubMed: 12588574]
15. Volpato S, et al. Predictive Value of the Short Physical Performance Battery Following Hospitalization in Older Patients. J Gerontol Ser A-Biol Sci Med Sci. 2011; 66:89–96. [PubMed: 20861145]
16. Croll NA, Smith J, Zuckerman BM. The aging process of the nematode Caenorhabditis elegans in bacterial and axenic culture. Exp Aging Res. 1977; 3:175–199. [PubMed: 334555]
17. Duhon SA, Johnson TE. Movement as an index of vitality – Comparing wild-type and the age-1 mutant of Caenorhabditis elegans. J Gerontol Ser A-Biol Sci Med Sci. 1995; 50:B254–B261. [PubMed: 7671016]
18. Herndon LA, et al. Stochastic and genetic factors influence tissue-specific decline in ageing *C. elegans*. Nature. 2002; 419:808–814. [PubMed: 12397350]
19. Huang C, Xiong CJ, Kornfeld K. Measurements of age-related changes of physiological processes that predict lifespan of Caenorhabditis elegans. Proc Natl Acad Sci U S A. 2004; 101:8084–8089. [PubMed: 15141086]
20. Glenn CF, et al. Behavioral deficits during early stages of aging in Caenorhabditis elegans result from locomotory deficits possibly linked to muscle frailty. J Gerontol Ser A-Biol Sci Med Sci. 2004; 59:1251–1260. [PubMed: 15699524]
21. Hsu AL, Feng ZY, Hsieh MY, Xu XZS. Identification by machine vision of the rate of motor activity decline as a lifespan predictor in C. elegans. Neurobiol Aging. 2009; 30:1498–1503. [PubMed: 18255194]
22. Garigan D, Hsu AL, Fraser AG, Kamath RS, Ahringer J, Kenyon C. Genetic analysis of tissue aging in Caenorhabditis elegans: a role for heat-shock factor and bacterial proliferation. Genetics. 2002; 161:1101–1112. [PubMed: 12136014]
23. Liu J, et al. Functional Aging in the Nervous System Contributes to Age-Dependent Motor Activity Decline in C. elegans. Cell Metab. 2013; 18:392–402. [PubMed: 24011074]
24. Crane JD, Devries MC, Safdar A, Hamadeh MJ, Tarnopolsky MA. The Effect of Aging on Human Skeletal Muscle Mitochondrial and Intramyocellular Lipid Ultrastructure. J Gerontol Ser A-Biol Sci Med Sci. 2010; 65:119–128. [PubMed: 19959566]
25. Johnson ML, Robinson MM, Nair KS. Skeletal muscle aging and the mitochondrion. Trends Endocrinol Metab. 2013; 24:247–256. [PubMed: 23375520]
26. Marzetti E, et al. Mitochondrial dysfunction and sarcopenia of aging: From signaling pathways to clinical trials. Int J Biochem Cell Biol. 2013; 45:2288–2301. [PubMed: 23845738]
27. Regmi SG, Rolland SG, Conradt B. Age-dependent changes in mitochondrial morphology and volume are not predictors of lifespan. Aging. 2014; 6:118–130. [PubMed: 24642473]
28. Sánchez-Blanco A, Kim SK. Variable Pathogenicity Determines Individual Lifespan in *Caenorhabditis elegans*. PLoS Genet. 2011; 7:e1002047. [PubMed: 21533182]
29. Lin K, Dorman JB, Rodan A, Kenyon C. daf-16: An HNF-3/forkhead family member that can function to double the lifespan of Caenorhabditis elegans. Science (New York, NY). 1997; 278:1319–1322.
30. Ryan DA, et al. Sex, Age, and Hunger Regulate Behavioral Prioritization through Dynamic Modulation of Chemoreceptor Expression. Curr Biol. 2014; 24:2509–2517. [PubMed: 25438941]
31. Samuelson AV, Carr CE, Ruvkun G. Gene activities that mediate increased lifespan of C. elegans insulin-like signaling mutants. Genes Dev. 2007; 21:2976–2994. [PubMed: 18006689]

32. Restif C, Ibanez-Ventoso C, Vora MM, Guo SZ, Metaxas D, Driscoll M. CeleST: Computer Vision Software for Quantitative Analysis of C. elegans Swim Behavior Reveals Novel Features of Locomotion. PLoS Comput Biol. 2014; 10:12.

33. Zeckhauser R, Shepard D. Where now for saving lives. Law Contemp Probl. 1976; 40:5–45.

34. Kauffman AL, Ashraf JM, Corces-Zimmerman MR, Landis JN, Murphy CT. Insulin signaling and dietary restriction differentially influence the decline of learning and memory with age. PLoS biology. 2010; 8:e1000372. [PubMed: 20502519]

35. Evans EA, Kawli T, Tan MW. Pseudomonas aeruginosa suppresses host immunity by activating the DAF-2 insulin-like signaling pathway in Caenorhabditis elegans. PLoS pathogens. 2008; 4:e1000175. [PubMed: 18927620]

36. Cohen E, Bieschke J, Perciavalle RM, Kelly JW, Dillin A. Opposing activities protect against age-onset proteotoxicity. Science (New York, NY). 2006; 313:1604–1610.

37. Mulcahy B, Holden-Dye L, O'Connor V. Pharmacological assays reveal age-related changes in synaptic transmission at the Caenorhabditis elegans neuromuscular junction that are modified by reduced insulin signalling. The Journal of experimental biology. 2013; 216:492–501. [PubMed: 23038730]

38. Luo S, Kleemann GA, Ashraf JM, Shaw WM, Murphy CT. TGF-beta and insulin signaling regulate reproductive aging via oocyte and germline quality maintenance. Cell. 2010; 143:299–312. [PubMed: 20946987]

39. Yang JS, et al. OASIS: Online Application for the Survival Analysis of Lifespan Assays Performed in Aging Research. PLoS One. 2011; 6:11.

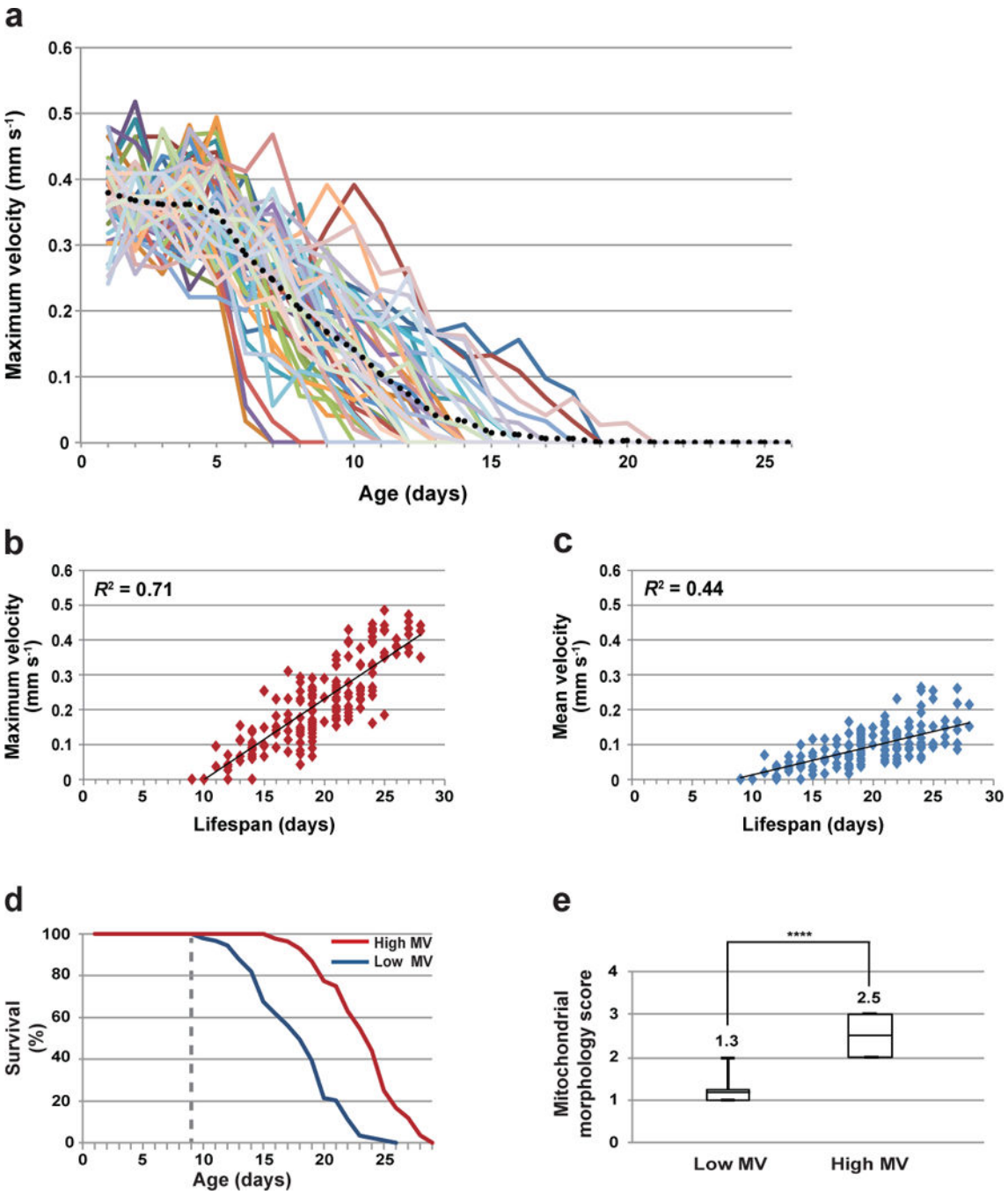

Figure 1. Maximum velocity (MV) is correlated with longevity

(**a**) Age-dependent changes in the MV of 52 individual wild type worms. Black dots represent the average value at each age. (**b**) and (**c**) Correlation between MV and lifespan (**b**) and correlation between mean velocity and lifespan (**c**) of individual worms. The MVs and mean velocity of the individual worms were measured at Day 9 of adulthood and their lifespan were measured thereafter. r^2, coefficient of determination. n = 173. (**d**) Survival curves of the low MV (n = 89) and high MV (n = 84) group worms. The groups were divided at Day 9 of adulthood (gray dot line) and the survivorship of worms in each group

was measured thereafter. (**e**) Correlation of MV with mitochondrial morphology at Day 9 of adulthood. Scores of mitochondrial morphology of low MV and high MV groups were 1.3 ± 0.5 and 2.5 ± 0.5, respectively (n = 27). The bottom and top of the box and whiskers are the first and third quartiles, and the band inside the box means average. Significance was determined using a two tailed, unpaired t-test. **** ($p < 0.0001$).

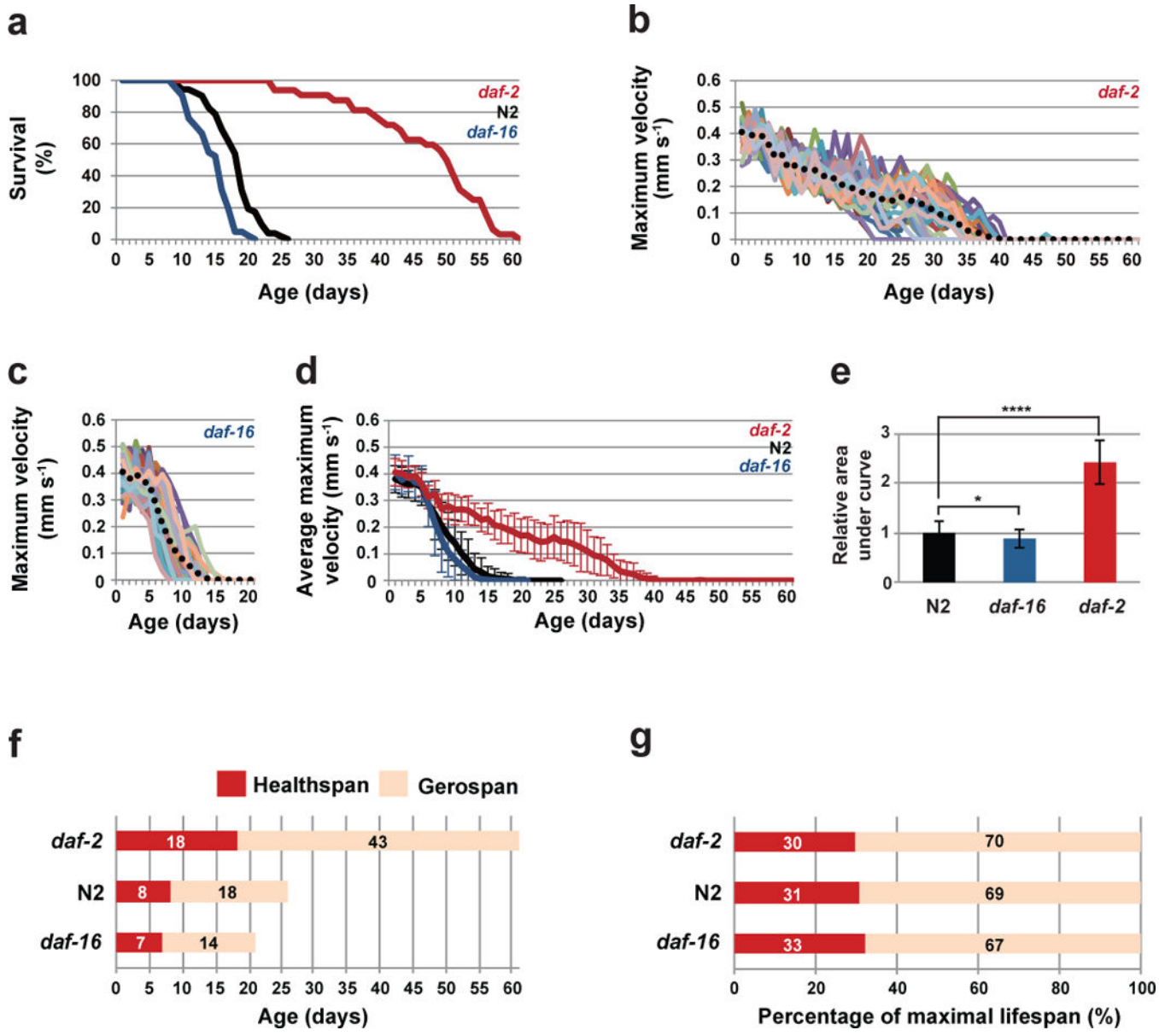

Figure 2. Correlation of MV with lifespan in *daf-2* mutants

(**a**) Age-associated change of survivorship in N2 (wild type) (n = 52), *daf-2(e1370)* (n = 32), and *daf-16(mu86)* (n = 42) worms. (**b**) and (**c**) Age-associated change of MVs in *daf-2* (**b**) and *daf-16* mutant worms (**c**). (**d**) Age-associated change of average MVs in N2 (n = 52), *daf-2* (n = 32) and *daf-16* (n = 42) mutant worms. Error bars represent s.d. (**e**) A cumulative difference in physical performance in N2 and *daf-16* and *daf-2* mutant worms as indicated by area under curves in (**d**). The relative values of area under curves are 1.0 ± 0.2, 0.9 ± 0.2, and 2.4 ± 0.4 for N2, *daf-16*, and *daf-2* worms, respectively. (**f**) Comparison of healthspan and gerospan in N2, *daf-16* and *daf-2* worms. Healthspan was defined as “the period during which the worm showed greater than 50% maximal functional capacity of wild type”[2]. Gerospan was defined as “the period during which the worm showed less than 50% maximal

functional capacity of wild type"[2]. (**g**) The normalized healthspan-to-gerospan ratio to their maximal lifespan in N2, *daf-16*, and *daf-2* worms.

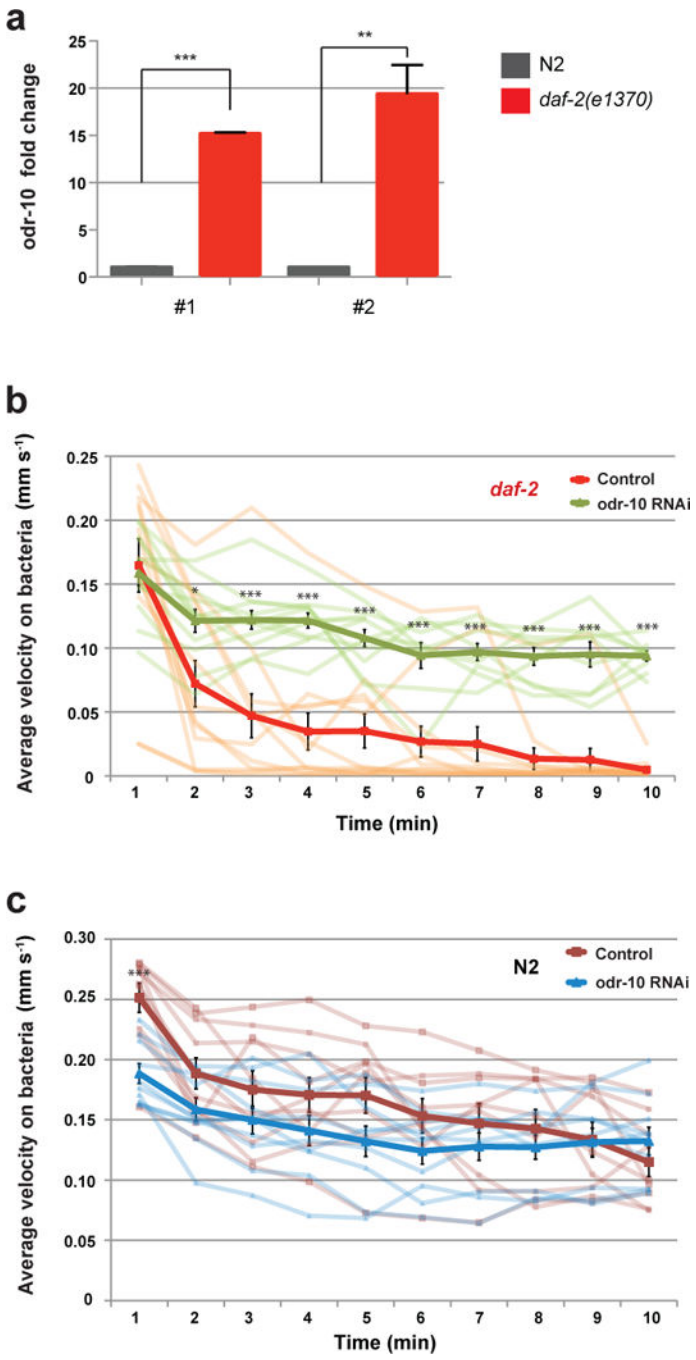

Figure 3. Motility on bacteria measures food preference rather than ability to move

(**a**) Two sets of primers (#1 and #2) were used to measure the expression of *odr-10* by qRT-PCR in N2 and *daf-2* mutants. For each primer set, *odr-10* expression in wild type was normalized to 1. *odr-10* expression in *daf-2* mutants increased by 15.2 ± 0.2 fold and 19.4 ± 3.1 fold, respectively. (**b**) Reduction of *odr-10* levels by RNAi increased *daf-2* motility on bacteria significantly. *daf-2* on OP50: 0.04 ± 0.03 mm/s; *daf-2; odr-10(RNAi):* 0.11 ± 0.01 mm/s **(c)** wild-type worms' motility on bacteria was not significantly affected by reduction

of *odr-10*: N2 worms on OP50: 0.17 ± 0.03 mm/s; N2 on *odr-10(RNAi):* 0.14 ± 0.03 mm/s. n=3, * ($p < 0.05$), ** ($p < 0.01$), *** ($p < 0.001$), **** ($p < 0.0001$); Unpaired t-test.

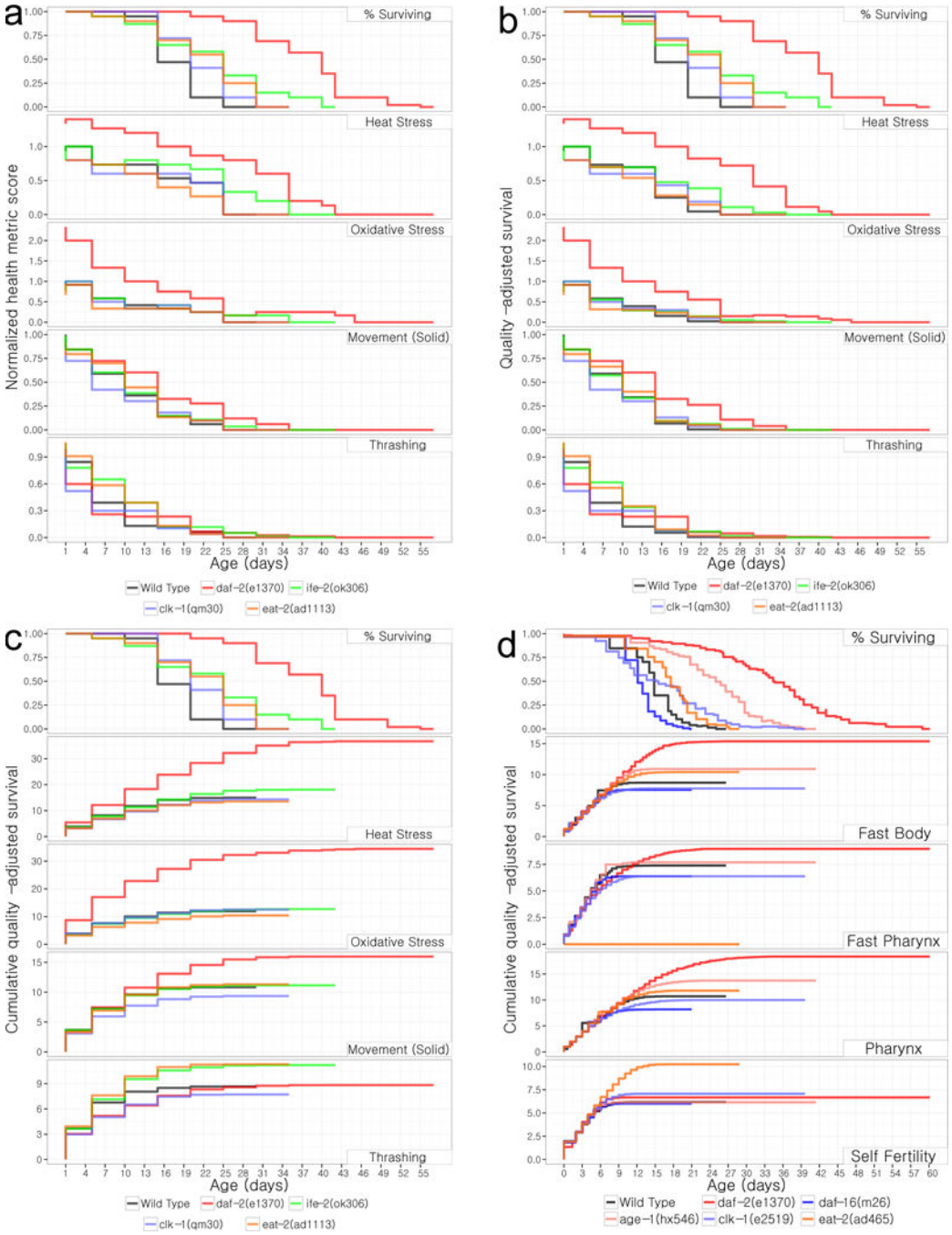

Figure 4. Quality-adjusted health metrics

daf-2 mutants are healthier than wild type. (**a**) Quality-adjusted lifespan curves for the health metrics observed by Bansal et al.[2], with each metric normalized to the maximum value of the wild type. (**b**) The Quality-adjusted lifespan curve is the survival rate multiplied by the normalized health measurement. (**c**) Visualizing the cumulative area under the quality-adjusted lifespan curve at each time point shows that *daf-2* mutants have higher lifespan quality over most measured health metrics. (**d**) Analysis of additional healthspan data

measured by Huang et al.[19] shows a similar increase in total lifespan quality of *daf-2* mutants over wild type.